J Mol Model (2011) 17:1061–1068
DOI 10.1007/s00894-010-0809-2

ORIGINAL PAPER

Nucleation and mobility model of Ag_n clusters adsorbed on perfect and oxygen vacancy MgO surfaces

Yongfei Liu · Yan Wang · Guangju Chen

Received: 22 March 2010 / Accepted: 12 July 2010 / Published online: 25 July 2010

Abstract The structures and energy properties for Ag_n (n= 1-8) metal clusters adsorbed on the perfect and oxygen vacancy MgO surfaces have been studied by using the DFT/UB3LYP method with an embedded cluster model. The nucleation and mobility model for the Ag_n (n=1-8) clusters on the perfect and oxygen vacancy MgO(100) surfaces was investigated. The results show that the Ag atoms locate initially at the surface oxygen vacancy sites; then, with the growth of Ag cluster sizes, the large Ag clusters move possibly out of the vacancy sites by a rolling model, and diffuse on the MgO surface under a certain temperature condition. The relative energies needed for moving out of the oxygen vacancy region for the adsorbed Ag_n clusters with the rolling model have been predicted. The even-odd oscillation behaviors for the cohesive energies, nucleation energies, first ionization potentials and HOMO-LUMO gaps of the adsorbed Ag_n clusters with the variation of cluster sizes have also been discussed.

Keywords Adsorbed Ag clusters · DFT/UB3LYP method · MgO surface · Mobile model

Introduction

In recent years, adsorbed properties of transition metal atoms or clusters supported on oxide surfaces have been shown to play a significant role in heterogeneous catalysis, deoxidization of nitrogen oxides, chemical sensors and so forth [1–5]. The choices of metal atoms and oxide substrates are crucial in order to get desired catalytic reactivity and selectivity. The catalytic activities of these catalysts have been known to depend on the metal cluster sizes, shape and adsorption sites. Growth of metal atoms on the MgO(001) surface is an important work, and understanding of the growth process is essential for the ultimate application of metal-oxide interfaces [6]. The metal-oxide interface has become a topic of great interest for experimental [7–10] and theoretical [11–19] investigations. The properties of some interface systems have been extensively addressed by a series of experiments [10, 20]. For example, Ag_n/MgO catalyst plays a key role in catalytic fields, and has potential application in new electronic materials [21–23]. Ag-MgO model system is one of the first metal-oxide systems studied by surface science techniques [24]. Moreover, some experiments have reported that transition metal clusters supported on the MgO surface have two different growth modes, i.e., three-dimensional (3D) and two-dimensional layer-by-layer (2D) modes [9, 25, 26]. A 2D or 3D configuration for a supported metal cluster refers to a monolayer or multilayer structure. The morphology of metal clusters depends on the strengths of interactions of metal-metal and metal-oxide interfaces. If the interaction of metal-metal interface is stronger than that of metal-oxide interface, the metal atoms tend to form 3D mode deposition, such as the Ag clusters deposited on the MgO surface [25, 27, 28]. Larsen et al. found that the Ag-MgO interaction was weak, and its growth mode presented the Volmer-Weber mode with 3D islands studied by Auger electron spectroscopy [27]. Schaffner et al. also employed x-ray photoelectron spectroscopy and electron-energy-loss spectroscopy to verify the 3D growth of Ag atoms on MgO surface [25]. On the other hand, MgO is a widely used oxide-substrate for metal catalysts [29], and has been greatly employed to study the

Y. Liu · Y. Wang (✉) · G. Chen (✉)
College of Chemistry, Beijing Normal University,
Beijing 100875, People's Republic of China
e-mail: wangy@bnu.edu.cn
e-mail: gjchen@bnu.edu.cn

properties of metal-substrate interface [30–32]. It has been found by previous experimental and theoretical studies that Fs type defects (i.e., neutral oxygen vacancy sites) of MgO (100) surface are not only trapping and nucleation centers for metal clusters, but also catalytic centers for adsorbates [32–34]. The Fs sites have been chosen to address the effect of the surface and simple oxygen vacancy on the absorption patterns of silver clusters [34–36].

Despite the rather intense experimental efforts that have been undertaken in recent years [1, 10], important details of metal-substrate interactions are unclear. Especially, some interaction properties at the metal-oxide interfaces, the atomic level structure at metal-oxide interfaces, the electronic characteristics of metal atoms deposited at oxide surface and thermodynamic stability are quite complicated and far from a complete understanding. The theoretical studies on growth mechanisms of some metal clusters at the metal-oxide interface have been performed in the past [37]. Some studies have theoretically reported the deposition properties of silver atoms/clusters on the MgO(001) surface [27, 38–41]. For example, Zhukovskii et al. have performed the studies of extensive deposition of the small Ag and Cu clusters by DFT calculations [42]. Barcaro et al. found that the structure and energetics of Ag_n clusters (n=2-10) adsorbed on a double vacancy neutral defect of MgO surface [43]. Moreover, the theoretical studies indicated that there is strong even-odd oscillation in the Ag cluster stability [43, 44]. Barcaro et al. have demonstrated some diffusion models of monomer hopping, dimmer leapfrog and trimer walking of Ag atoms on the MgO surface [45]. The Ag clusters deposited on the MgO surface can diffuse quickly even at low temperatures [3, 11, 45, 46]. Therefore, it can be seen from these studies that to understand the mechanism of diffusion, aggregation and mobility of Ag clusters on the MgO surface is very important. Although many contributions have been provided to this field [38], a systematically study on Ag atom nucleation and mobility modes on perfect and oxygen vacancy MgO surfaces is still lacking. So, the main goals of this paper are (1) to clarify structural parameters and energy properties of Ag clusters supported on the perfect and oxygen vacancy MgO surfaces; (2) to identify the mechanism of growth and mobility for Ag clusters on the MgO surface; (3) to address a rolling mechanism of Ag cluster mobility out of oxygen vacancy region with detail energetic information.

Computational details and models

The embedded quantum cluster of $Mg_{31}O_{22}$ consisting of both oxygen center and oxygen vacancy site of MgO(100) surface provides the substrate for the supported Ag_n (n= 1-8) clusters, as shown in Fig. 1. The quantum mechanical region is treated by the DFT/UB3LYP method. Effects of

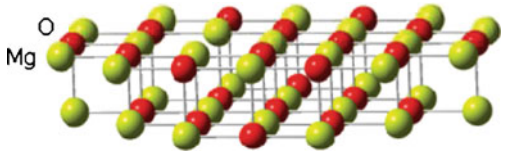

Fig. 1 Quantum cluster model of $Mg_{31}O_{22}$

sizes of the MgO clusters on the studied system properties have been estimated by the results in the surface binding (SBD) energy for the adsorption of single Ag adatom on the thicker MgO cluster by two more layers, and in the SBD energy per atom for the adsorption of Ag_8 cluster on the larger MgO cluster by 12 atoms more than the original one, respectively. The results indicate that the SBD energy differences per atom calculated by the three types of MgO clusters are in the range of 5%. Therefore, the current $Mg_{31}O_{22}$ cluster has been chosen as a substrate for this study. A small electron core potential, Hay-Wadt ECP and double-ζ plus polarization basis sets for valence electrons have been employed for Ag atoms, which explicitly includes 19-valence-electrons ($4s^2 4p^6 4d^{10} 5s^1$) effective-core potential. For other selected basis sets, the 6-31++G (d) basis set has been used for the Mg atoms nearest the vacancy to describe the electron localization in the cavity. The 6-31G (d) basis set was used for selected Mg and O atoms close to the adsorption centers. The 3-21G basis set was used for the remaining MgO cluster atoms. These selected basis sets have been tested by many previous studies to describe correctly the metal clusters on MgO surface [47–49]. The geometries of the adsorbed Ag clusters and some nearest surface atoms, i.e., the four magnesium atoms or one oxygen atom and four magnesium atoms close to the adsorption centers on the surface are fully optimized. The basis set superposition errors (BSSE) for all systems have been corrected by using the full counterpoise method of Boy and Bernardi [50]. The values of BSSE per atom for all clusters are in a range of 5.8~ 6.6 kcal mol^{-1}. To simulate infinite crystal Madelung potential field, the embedded quantum cluster is surrounded by a set of point charges whose unit cell was within 1.2 nm from any of the quantum cluster atoms and a set of total ion model potentials (TIMPs) for all Mg^{2+} ions that are nearest to any quantum oxygen atom. These point charges (PC = ±2) and TIMPs are located at the lattice positions, which are taken from the experimental MgO bulk structure. With these TIMPs the artificial polarization of oxygen anions at the cluster borders can be reduced and the orthogonality condition between the cluster orbitals; and the orbitals of the crystal surrounding can be effectively included. The Madelung potential from the remaining extended MgO surface is represented by a set of surface charges derived from the surface charge representation of the external embedded potential (SCREEP) method. More

details about the SCREEP method can be found elsewhere [49, 51, 52]. All calculations were carried out by using the GAUSSIAN03 program [53].

The isolated Ag atom exhibits the ground electron configurations of $4d^{10}5s^1$. The ground spin state with $^2S_{1/2}$ has been tested for the isolated Ag atom [54]. In the following section, we investigated the possibility of variation of the spin states for Ag atoms upon adsorption on both perfect and oxygen vacancy MgO surfaces.

Results and discussion

Structures of adsorbed Ag clusters

In this section we present the geometric parameters for the most stable structures of supported Ag_n (n=1-8) clusters on Fs centers and the perfect MgO surface with 3D configurations based on the previous studies [55]. The initial structures of some Ag_n clusters for geometrical optimizations were referenced from the previous work [27, 55, 56]. The most stable structures of the clusters were recorded in the average adsorbate-substrate distance and Ag-Ag distance between adsorbed Ag atoms. Figure 2 describes the most stable structures for the Ag_n (n=5-7) clusters adsorbed on the oxygen vacancy MgO surfaces. The results show that one Ag atom in each cluster is always localized on the top of the oxygen vacancy site or the surface oxygen atom, and the other Ag atoms are bound around this central Ag atom on the surface to form a 3D cluster. The corresponding optimized values of the geometric parameters are shown in Table 1. The structures of Ag_n clusters supported on the perfect surface are the similar as those on the vacancy surfaces, except that Ag-O_{5c} average distances are larger about 0.2 Å than Ag-Fs ones. For example, the Ag-Fs bonding length of 2.30 Å for Ag_3 cluster adsorbed closer to the vacancy site is shorter than the Ag-O bonding length of 2.51 Å on the perfect surface. This is in line with all previous calculations [27, 38, 57]. In general, the structures of Ag_n clusters supported and those in the gas-phase have similar structures [58], except that average bond lengths of Ag clusters adsorbed on the surface are elongated with respect to those in the gas phase. On the other hand, there is no change of the ground spin state of adsorbed clusters with respect to those in the gas phase. Namely, the ground spin state is singlet state for the clusters with an even number of atoms. However, the ground spin state is doublet state for the clusters with an odd number of atoms. The spin state values for the electronic ground states of free Ag_n clusters are the same as the adsorbed Ag_n clusters.

Even-odd oscillation behaviors of adsorbed Ag_n clusters

The cohesive energies, nucleation energies, first ionization potentials and HOMO-LUMO gaps of Ag_n clusters adsorbed on the perfect and oxygen vacancy MgO surfaces present even-odd oscillation behaviors. The cohesive energy (E_{COH}) per atom and nucleation energy (E_{nuc}) were calculated as follows:

$$E_{COH}(per\ atom) = \frac{1}{n}[E(M_n) - nE(M)] \quad (1)$$

$$Enuc = \{E(M_n/MgO) - [E(M) + E(M_{n-1}/MgO)]\}. \quad (2)$$

Where M is an Ag atom, n is the number of Ag atoms in a cluster. M_n/MgO is a silver cluster and MgO surface with the geometry that was optimized. M_n is a silver cluster with the same geometry on the MgO surface. The COH energy

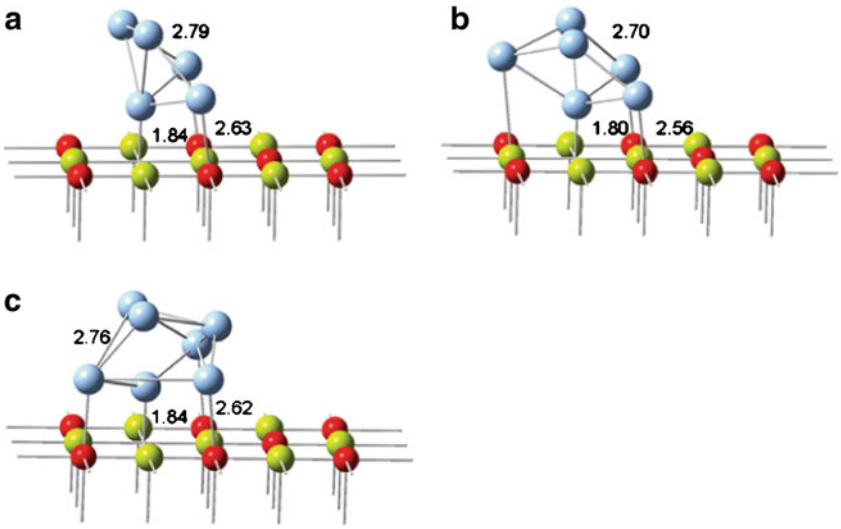

Fig. 2 Optimized geometries of Ag_n (n=5-7) (**a**-**c**)clusters adsorbed on the oxygen vacancy sites of MgO surface. Selected distances are given in Å

Table 1 Calculated average bond lengths (Å) of Ag clusters on three types of surface regions

		Oxygen center	Vacancy region	Rolling model
Ag_1	Ag-Surf.	2.54	2.06	2.88
Ag_2	Ag-Surf.	2.36	1.88	2.83
	Ag-Ag	2.61 (2.58)[a]	2.70	2.65
Ag_3	Ag-Surf.	2.51	2.30	2.82
	Ag-Ag	2.84 (2.82)[a]	2.74	2.75
Ag_4	Ag-Surf.	2.43	2.21	2.94
	Ag-Ag	2.71 (2.73)[a]	2.70	2.73
Ag_5	Ag-Surf.	2.52	2.36	2.63
	Ag-Ag	2.82	2.72	2.76
Ag_6	Ag-Surf.	2.50	2.18	2.48
	Ag-Ag	2.78	2.76	2.76
Ag_7	Ag-Surf.	2.53	2.34	2.48
	Ag-Ag	2.79	2.76	2.74
Ag_8	Ag-Surf.	2.53	2.39	2.45
	Ag-Ag	2.78	2.77	2.76

[a] is taken from reference [27]

describes the strength of metal-metal interaction. The nucleation energy (E_{nuc}) represents the binding energy of an Ag atom to a bound Ag cluster. The first ionization potential (IP) and HOMO - LUMO gap (HLG) are defined as follows:

$$IP = -E(HOMO) \tag{3}$$

$$E(HLG) = E(HOMO) - E(LUMO). \tag{4}$$

Where E(HOMO) and E(LUMO) are defined as the energies of highest occupied molecular orbital (HOMO) and lowest unoccupied molecular orbital (LUMO). The IP's were computed using Koopmans' theorem [59]. It is well known that the kinetic stability of a system is governed by the HOMO-LUMO gap. The larger the gap; the more stable the system.

Figure 3 shows the cohesive energies, nucleation energies, first ionization potentials and HOMO-LUMO gaps for the Ag_n clusters adsorbed on the oxygen vacancy MgO surface. Especially, the average energies for three types of structure configurations separately for Ag_5, Ag_6, Ag_7, and Ag_8 clusters have been reported since the three types for each of these clusters present similar stability. All energy curves in Fig. 3 present the characteristics of even-odd oscillation which means that the magnitudes of energy values for the even-numbered clusters are larger than those for the adjacent clusters. For example, it can be seen that the COH energy for Ag_6 is larger than those by 4.4 kcal mol^{-1} for the Ag_5 and by 2.5 kcal mol^{-1} for Ag_7. Additionally, the even-numbered clusters have larger HOMO–LUMO gaps than the odd-numbered neighbors. These results indicate that even-numbered adsorbed Ag_n clusters are relatively more stable than the neighboring odd-numbered Ag_n clusters. Especially, the nucleation energies and the first ionization potentials present more obvious characteristics of even-odd oscillations. For even-numbered adsorbed Ag clusters, all the electrons in the clusters are paired with closed shell electron states, and their HOMOs are occupied by two electrons. However, the odd-numbered adsorbed Ag_n clusters have open-shell electronic configurations, and their SOMOs are occupied by one electron. The characteristics of even-odd oscillations result from the even-odd oscillations related to the intrinsic electronic nature of the layer opened/closed for clusters with odd and even n. In other words, odd - even oscillation behaviors can be understood by the effect of electron pairing in orbitals [60].

Nucleation and cluster growth of Ag_n clusters

In order to address nucleation, growth and mobility mechanism of the Ag_n clusters adsorbed on MgO surface, we have also analyzed the surface binding energy (SBD) per atom for these stable structures as follows:

$$E_{SBD}(per\ atom) = \frac{1}{n}\{E(M_n/MgO) - [E(MgO) + E(M_n)]\}. \tag{5}$$

The SBD energies represent the strength of the interaction between the metal atoms and the MgO substrate. Figure 4a, b show the SBD and COH energies per atom with BSSE corrections for the Ag_n clusters adsorbed on the oxygen vacancy and perfect MgO surfaces, respectively. Although the bindings of Ag atoms to the MgO surface present much weak interaction, we can propose a physical

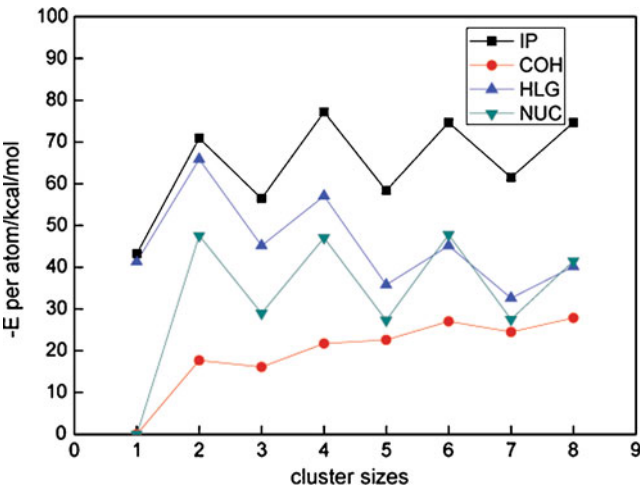

Fig. 3 Calculated COH energies per atom, nucleation energies per atom, HOMO-LUMO gaps and first ionization energies of Ag clusters supported on the oxygen vacancy MgO surface

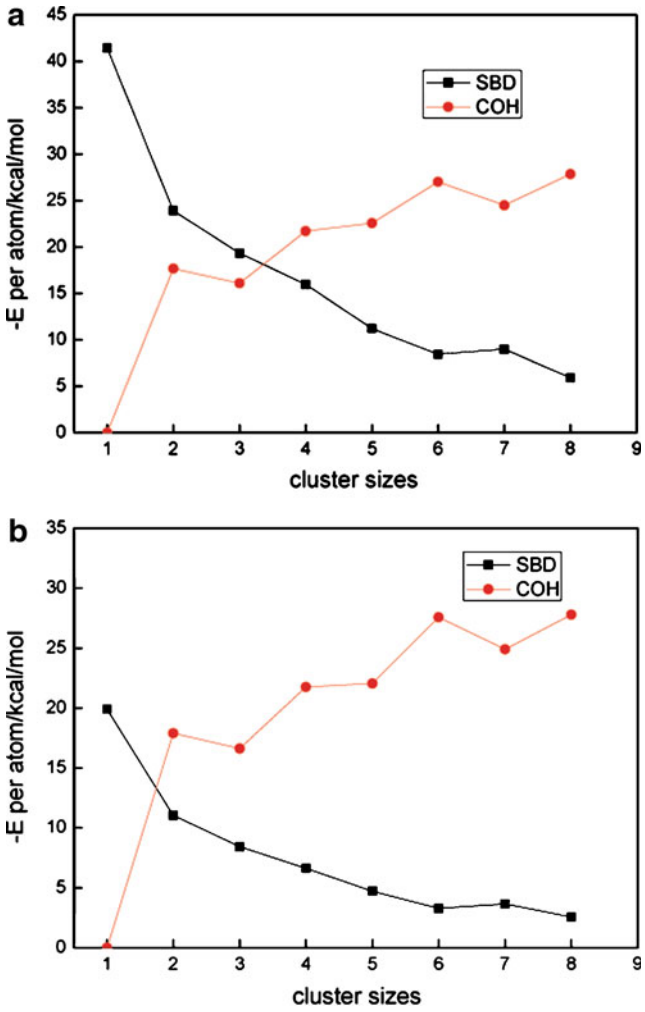

Fig. 4 The SBD and COH energies per atom of Ag clusters on the oxygen vacancy (**a**) and perfect (**b**) MgO surface

picture of nucleation and cluster growth process from the calculated energy trends for Ag clusters on MgO surface. It can be seen from Fig. 4 for both types of MgO surfaces that the SBD energies per atom generally decrease from Ag_1 to $Ag_{8;}$ in contrast, the COH energies per atom increase with the increase of Ag cluster sizes. For example, for the oxygen vacancy MgO surface, the magnitudes of SBD energies per atom decrease in the order of Ag_1 (41.4 kcal mol^{-1}) > Ag_2 (24.0 kcal mol^{-1}) > Ag_3 (19.0 kcal mol^{-1}) > Ag_4 (16.0 kcal mol^{-1}) > Ag_5 (11.2 kcal mol^{-1}) > $Ag_6 \approx Ag_7$ (average 8.8 kcal mol^{-1}) > Ag_8(6.0 kcal mol^{-1}) (see Fig. 4a). Oppositely, the magnitudes of COH energies per atom on the oxygen vacancy MgO surface increase gradually in the order of $Ag_2 \approx Ag_3$ (average 17.0 kcal mol^{-1}) < Ag_4 (21.7 kcal mol^{-1}) < Ag_5 (22.6 kcal mol^{-1}) < Ag_6 (27.0 kcal mol^{-1}) > Ag_7 (24.5 kcal mol^{-1}) < Ag_8 (27.8 kcal mol^{-1}) (see Fig. 4a). Similar trends have been found for these clusters on the perfect MgO surface (see Fig. 4b). Therefore, according to these energy trends, the process of nucleation and growth of Ag clusters on the MgO surface can be briefly described as follows. The Ag atoms locate initially at the surface oxygen vacancy sites and grow up gradually around the vacancy sites due to the large magnitudes of the SBD energies on the oxygen vacancy sites of MgO surface with respect to on the perfect surface. Then, due to the chemical interactions between the metal atoms, the COH energies per atom with even-odd alterative behavior generally increase with the increase of Ag cluster sizes on the oxygen vacancy MgO surface. The large magnitudes of the COH energies for the big clusters are dominant and driving forces for their growth on the MgO surface. Furthermore, with the growth of Ag clusters, the large Ag clusters move possibly out of the vacancy sites thermodynamically, because the SBD energy differences between Ag clusters adsorbed on the oxygen vacancy sites and those on the oxygen centers of perfect MgO surface decrease with the increase of the cluster sizes. For example, as shown in Fig. 5, such SBD energy difference per atom of 21.54 kcal mol^{-1} for Ag_1 atom decreases to 3.37 kcal mol^{-1} for Ag_8 cluster. More details about the cluster formation model can be found elsewhere [61, 62]. Moreover, although the cohesive energies, nucleation energies, first ionization potential and HOMO-LUMO gaps with cluster size n show even-odd alterative behaviors on the MgO surfaces, the variation tendency of the SBD energies still decreases constantly, and the increased trend of the COH energies of adsorbed Ag_n clusters is also presented with instant submerging of even-odd oscillation as the cluster sizes increase. These results indicate that the even-odd oscillation behavior of Ag clusters does not affect the cluster formation process of Ag atoms on the MgO surface.

Rolling mobility mechanism of adsorbed Ag clusters

Expecting the mobility of the big adsorbed Ag clusters from the vacancy sites, the structures and energies of Ag_n

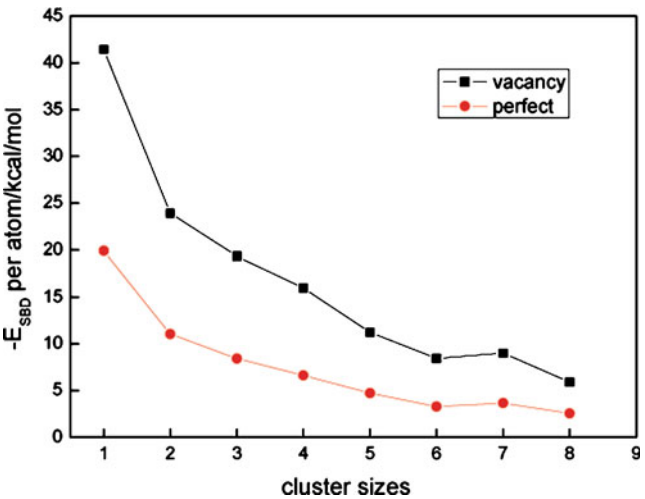

Fig. 5 The differences of SBD energies per atom between oxygen center and oxygen vacancy site of MgO surface for Ag clusters

clusters for a rolling movement model have been investigated thermodynamically. The Ag_n (n=1-8) cluster structures adsorbed at the middle of vacancy and perfect surface regions have been optimized with the distances of Ag atoms connecting to the surface atoms relaxed, and the Ag_n cluster shapes fixed relatively. The optimized structures and geometric parameters of only one type of Ag_8 clusters at the perfect surface, the vacancy site and the middle of the vacancy and terrace regions have been separately shown in Fig. 6 and Table 1. As shown in Fig. 6, the Ag1 and Ag2 atoms originally localized at the bottom of the Ag_8 cluster around the vacancy region move to the top of the cluster at the middle region; and at the same time, the corresponding Ag5 and Ag8 atoms originally localized at the top of the cluster on the vacancy region move to the bottom of the cluster at the middle region. This structure of the Ag_8 cluster at the middle region presents the characteristics of the rolling process. As expected, the energies of Ag_n clusters at the middle of vacancy and terrace regions are generally higher than those on the perfect surface and vacancy region. In particular, the average energy differences per atom at the middle of the vacancy and terrace regions with respect to the vacancy region are shown in Fig. 7 and present in the order of 16.00 kcal mol^{-1}, 11.96 kcal mol^{-1}, 8.44 kcal mol^{-1}, 8.09 kcal mol^{-1}, 6.67 kcal mol^{-1}, 5.38 kcal mol^{-1} and 5.21 kcal mol^{-1} for Ag_2, Ag_3, Ag_4, Ag_5, Ag_6, Ag_7 and Ag_8 with the rolling model, respectively. Such relative energy values for these adsorbed Ag_n clusters (shown in Fig. 7) provide a possible estimation for the energies needed for the clusters rolling out of the vacancy sites. The gradual decrease of such energy differences with the increase of the cluster sizes predicts the tendency of big Ag_n clusters easily moving out of the vacancy sites. Therefore, it is possible that the big metal clusters move out of the vacancy region at a certain temperature condition in experiments besides single atom or some atoms detaching from the clusters. That is, because the probability of the diffusive event is a function of the external temperature, the diffusion of the clusters with sufficiently low barrier can occur at a relatively low temperature [63]. These results can be comparable to the barrier range of 2~6 kcal mol^{-1} which are needed for the diffusion models of hopping, leapfrog, and walking for small adsorbed Ag_n clusters on the perfect MgO surface, which was studied by Barcaro et al. [45]. It is clear that the barriers from vacancy sites to a perfect surface are expected larger than those for the cluster diffusion on a perfect surface.

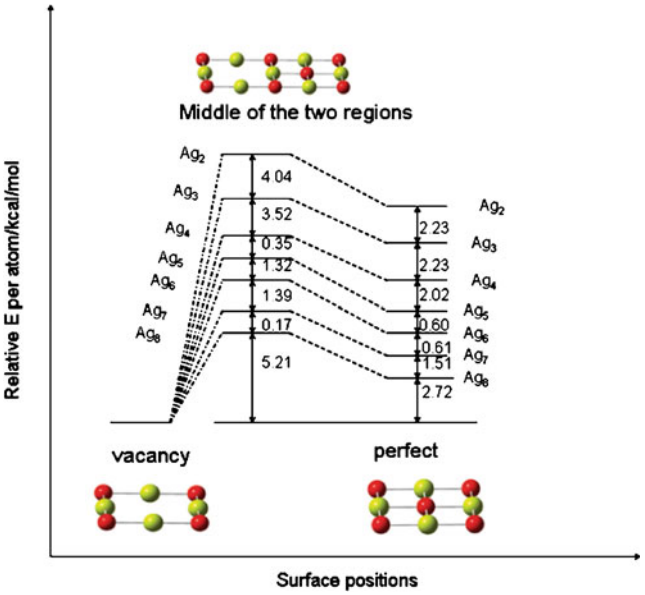

Fig. 7 Scheme of the relative energies of Ag clusters on the oxygen vacancy site, the middle of vacancy and terrace regions and the terrace region

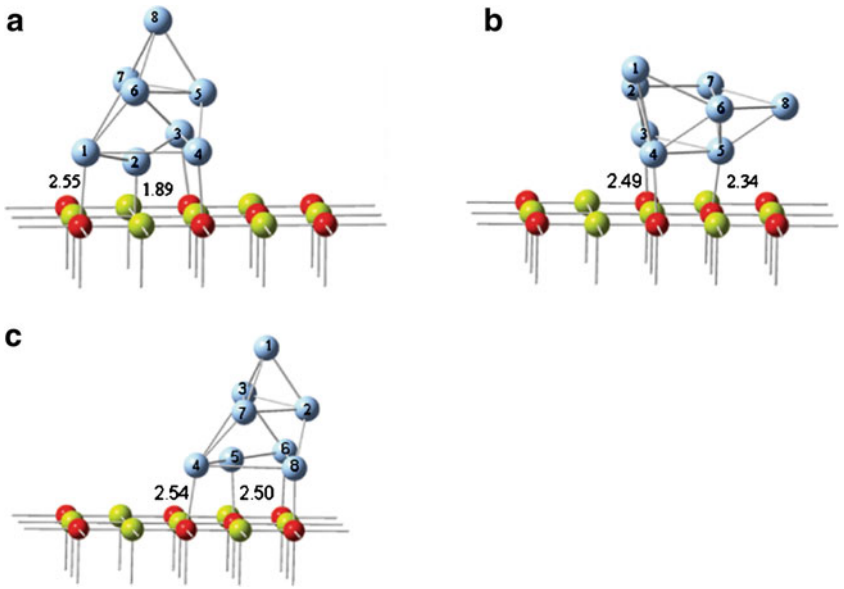

Fig. 6 Optimized geometries of Ag_8 : (**a**) on the oxygen vacancy site, (**b**) on the middle of vacancy and terrace regions for rolling model and (**c**) on the oxygen center. Selected distances are given in Å

Conclusions

The study of nucleation and mobile model for small Ag_n (n= 1-8) clusters on the perfect and oxygen vacancy MgO(100) surfaces are performed based on the DFT/UB3LYP method and embedded cluster model. As expected, the even-odd oscillation behaviors of cohesive energies, nucleation energies, first ionization potentials, and HOMO-LUMO gaps have been found for the adsorbed Ag_n clusters with cluster size variation. The cluster formation process of adsorbed Ag_n clusters with the even-odd oscillation character and weak interface interaction for Ag_n clusters on MgO surface has been predicted. Namely, the Ag atoms locate initially at the surface oxygen vacancy sites. With the growth of Ag cluster sizes, the large Ag clusters move possibly out of the vacancy sites and diffuse on the MgO surface by the rolling model under a certain temperature condition. Otherwise, the reasonable and relative energy of average 6.28 kcal mol^{-1} per atom between the vacancy and the middle of vacancy and terrace regions for adsorbed Ag_n (n>4) clusters presents the possibility of moving out of the oxygen vacancy region with the rolling model. Such favorable small energies for moving out of vacancy region for Ag_n clusters on MgO surface result from the weak adsorbates-substrate interface and great adsorbate-adsorbate interaction. These results provide an insight into understanding the nucleation and growth processes of metal clusters on the MgO surface.

Acknowledgments We are grateful to thank Prof. Thanh N. Truong from University of Utah for his useful suggestions and valuable work on this paper. This work is supported by the National Science Foundation of China (No. 20771017, 20973024, 20673011 and 20631020), the Major State Basic Research Development Programs (grant No. G2004CB719900).

References

1. Lim DC, Lopez-Salido I, Kim YD (2005) Surf Sci 598:96–103
2. Freund H (2002) Surf Sci 500:271–299
3. Yudanov I, Pacchioni G, Neyman K, Rosch N (1997) J Phys Chem B 101:2786–2792
4. Hutchings GJ, Haruta M (2005) Appl Catal A 291:2–5
5. Lu NX, Fu G, Xu X, Wan HL (2008) J Chem Phys 128:034702–034709
6. Suzuki T, Hishita S, Oyoshi K, Souda R (1999) Surf Sci 442:291–299
7. Stuckless JT, Starr DE, Bald DJ, Campbell CT (1997) J Chem Phys 107:5547–5553
8. Barbier A, Renaud G, Jupille J (2000) Surf Sci 454–456:979–983
9. Larsen JH, Ranney JT, Starr DE, Musgrove JE, Campbell CT (2001) Phys Rev B 63:195410-1–195410-8
10. Lopez-Salido I, Lim DC, Dietsche R, Bertram N, Kim YD (2006) J Phys Chem B 110:1128–1136
11. Barcaro G, Fortunelli A (2005) J Chem Theor Comput 1:972–985
12. Dong YF, Wang SJ, Mi YY, Feng YP, Huan ACH (2006) Surf Sci 600:2154–2162
13. Barcaro G, Fortunelli A (2008) Chem Phys Lett 457:143–147
14. Wang SG, Li YW, Jiao H, Lu JX, He MY (2004) J Phys Chem B 108:8359–8363
15. di Valentin C, Scagnelli A, Pacchioni G, Risse T, Freund HJ (2006) Surf Sci 600:2434–2442
16. Fuks D, Zhukovskii YF, Kotomin EA, Ellis DE (2006) Surf Sci 600:L99–L104
17. Goniakowski J, Jelea A, Mottet C, Barcaro G, Fortunelli A, Kuntova Z, Nita F, Levi AC, Rossi G, Ferrando R (2009) J Chem Phys 130:174703–174709
18. Lu X, Xu X, Wang N, Zhang Q (1999) J Phys Chem B 103:3373–3379
19. Ferrando R, Rossi G, Levi AC, Kuntova Z, Nita F, Jelea A, Mottet C, Barcaro G, Fortunelli A, Goniakowski J (2009) J Chem Phys 130:174702–174709
20. Renaud G (1998) Surf Sci Rep 32:5–90
21. Zheng J, Petty JT, Dickson RM (2003) J Am Chem Soc 125:7780–7781
22. Zheng J, Dickson RM (2002) J Am Chem Soc 124:13982–13983
23. Lee T, Dickson RM (2003) J Phys Chem B 107:7387–7390
24. Palmberg PW, Rhodin TN, Todd CJ (1967) Phys Rev Lett 11:33–35
25. Schaffner MH, Patthey F, Schneider WD (1998) Surf Sci 417:159–167
26. Robach O, Renaud G, Barbier A (1999) Phys Rev B 60:5858–5871
27. Hu Y, Zhang W, Deng Y, Tang B (2008) Comput Mater Sci 42:43–49
28. Trampert A, Ernst E, Flynn CP, Fischmeister HF, Ruhle M (1992) Acta Metall Mater 40:S227–S236
29. Duriez C, Chapon C, Henry CR, Rickard JM (1990) Surf Sci 230:123–136
30. Verdozzi C, Jennison DR, Schultz PA, Sears MP (1999) Phys Rev Lett 82:799–802
31. Campbell CT (1997) Surf Sci Rep 27:1–111
32. Henry CR (1998) Surf Sci Rep 31:231–325
33. Pacchioni G, Pescarmona P (1998) Surf Sci 412–413:657–671
34. Shibata T, Bunker BA, Zhang Z, Meisel D, Vardeman CF, Gezelter JD (2002) J Am Chem Soc 124:11989–11996
35. Haas G, Menck A, Brune H, Barth JV, Venables JA, Kern K (2000) Phys Rev B 61:11105–11108
36. Del Vitto A, Sousa C, Illas F, Pacchioni G (2004) J Chem Phys 121:7457–7466
37. Fuks D, Dorfman S, Zhukovskii YF, Kotomin EA (2002) Marshall Stoneham A. Surf Sci 499:24–40
38. Zhukovskii YF, Kotomin EA, Jacobs PWM, Stoneham AM, Harding JH (1999) Surf Sci 441:373–383
39. Purton JA, Bird DM, Parker SC, Bullett DW (1999) J Chem Phys 110:8090–8097
40. Herschend B, Hermansson K, Alfredsson M, Zhukovskii YF, Kotomin EA, Jacobs PWM (2003) J Phys Chem B 107:11893–11899
41. Ferrari AM (2004) Chem Phys Lett 400:541–547
42. Zhukovskii YF, Kotomin EA, Fuks D, Dorfman S (2004) Superlattices Microstruct 36:63–72
43. Barcaro G, Fortunelli A (2007) Phys Rev B 76:165412-1–165412-6
44. Fournier R (2001) J Chem Phys 115:2165–2177
45. Barcaro G, Fortunelli A (2007) New J Phys 9:22–22
46. Benia HM, Nilius N, Freund HJ (2006) Surf Sci 600:128–133
47. Wang Y, Florez E, Mondragon F, Truong TN (2006) Surf Sci 600:1703–1713
48. Wang Y, Truong TN (2008) J Phys Chem C 112:13674–13680
49. Wang Y, Truong TN (2004) J Phys Chem B 108:3289–3294
50. Boys SF, Bernardi F (1970) Mol Phys 19:53
51. Stefanovich EV, Truong TN (1998) J Phys Chem C 102:3018–3022
52. Stefanovich EV, Truong TN (1996) J Chem Phys 104:2946–2955
53. Frisch MJ, Trucks GW, Schlegel HB, Scuseria GE, Robb MA, Cheeseman JR, Montgomery JA, Vreven JT, Kudin KN, Burant JC, Millam JM, Iyengar SS, Tomasi J, Barone V, Mennucci B, Cossi M, Scalmani G, Rega N, Petersson GA, Nakatsuji H, Hada M, Ehara M,

Toyota K, Fukuda R, Hasegawa J, Ishida M, Nakajima T, Honda Y, Kitao O, Nakai H, Klene M, Li X, Knox JE, Hratchian HP, Cross JB, Adamo C, Jaramillo J, Gomperts R, Stratmannv RE, Yazyev O, Austin AJ, Cammi R, Pomelli C, Ochterski JW, Ayala PY, Morokuma K, Voth GA, Salvador P, Dannenberg JJ, Zakrzewski VG, Dapprich S, Daniels AD, Strain MC, Farkas O, Malick DK, Rabuck AD, Raghavachari K, Foresman JB, Ortiz JV, Cui Q, Baboul AG, Clifford S, Cioslowsk IJ, Stefanov BB, Liu G, Liashenko A, Piskorz P, Komaromi I, Martin RL, Fox DJ, Keith T, Al-Laham MA, Peng C, Nanayakkara A, Challacombe M, Gill PMW, Johnson B, Chen W, Wong MW, Gonzalez C, Pople JA (2003) Gaussian 03, Revision B04. Gaussian Inc, Pittsburgh, PA

54. Neyman KM, Inntam C, Matveev AV, Nasluzov VA, Rosch N (2005) J Am Chem Soc 127:11652–11660
55. Barcaro G, Apra E, Fortunelli A (2007) Chem Eur J 13:6408–6418
56. Bonacic-Koutecky V, Urgel CB, Kronik L, Kuznetsov AE, Mitric R (2007) Eur Phys J 45:471–476
57. Giovanardi C, di Bona A, Moia TS, Valeri S, Pisani C, Sgroi M, Busso M (2002) Surf Sci 505:L209–L214
58. Zhao S, Liu Z, Li Z, Wang W, Fan K (2006) J Phys Chem A 110:11537–11542
59. Phillips JC (1961) Phys Rev 123:420–424
60. Deka A, Deka RC (2008) J Mol Struct 870:83–93
61. Xu L, Campbell CT, Jonsson H, Henkelman G (2007) Surf Sci 601:3133–3142
62. Venables JA, Haas G, Brune H, Harding JH (1999) Mat Res Soc Symp Proc 570:51–60
63. Musolino V, Selloni A, Car R (1999) Phys Rev Lett 83:3242–3245